Combining direct imaging of blended data and data-space deblending using a pattern-based approach

Joseph Jennings, Biondo Biondi, Robert Clapp and Shuki Ronen, Stanford University*

SUMMARY

We present a new algorithm for directly imaging blended data via waveform inversion. The algorithm relies on performing a data-space deblending step at each iteration of the waveform inversion. Following a pattern-based approach, this data-space deblending step is done through independent modeling of the source wavefields on which filters can be estimated and used to deblend the blended data. As the velocity model is updated, the filters will be estimated on increasingly more accurate data and therefore will provide improved deblending results from iteration to iteration. We show that with the introduction of these filters, the waveform inversion results contain significantly fewer artifacts than those obtained with conventional waveform inversion of blended data.

INTRODUCTION

Simultaneous source deblending

Reducing the acquisition time of seismic surveys by reducing the amount of time between shots of source vessels has shown to be very cost-efficient and also can provide better seismic imaging results (Beasley et al., 1998; Berkhout, 2008; Soni and Verschuur, 2015). This method, known as simultaneous sourcing, or blending, has been successfully implemented for large seismic exploration surveys and is now increasingly more common in seismic acquisition (Abma et al., 2012; Kommedal et al., 2016). While simultaneous sourcing does provide a decrease in acquisition time, it also introduces an overlap between shots that must be dealt with in the processing and imaging of these blended data.

Direct imaging of blended data

There are two methodologies for obtaining seismic images of blended data. One is to first separate the overlapped shots and then image the separated data. This approach has been widely studied and has provided high quality imaging results (Abma and Yan, 2009). The other, less-studied approach is to directly image these blended data by way of waveform inversion (Tang et al., 2009). While this approach has shown promise, it requires many iterations of inversion in order to mitigate the artifacts introduced in the imaging due to the cross-talk between sources (Leader, 2015). In some cases, depending on the extent of blending, these artifacts may remain even after many iterations of waveform inversion leading to poor-quality seismic images.

Previous studies on direct imaging of blended data have been successful in mitigating these artifacts by introducing a regularization term to the waveform inversion objective function (Xue et al., 2014; Chen et al., 2017). While effective, these approaches require a priori knowledge of the subsurface model (i.e., practitioners must make a choice of how to style the estimated model). In this work, we present an algorithm that does not require regularization of the model parameters but still results in minimal artifacts in the inverted model. The key to our approach is an inexpensive data-space deblending step based on a pattern-based method that is performed at each iteration of the waveform inversion.

Pattern-based approach using prediction-error filters (PEFs)

Pattern-based approaches separate signal and noise using the fact that the multidimensional spectra of the signal and the noise differ. These approaches have been successfully used in multiple removal, ground-roll attenuation and other coherent noise removal applications (Manin and Spitz, 1995; Brown et al., 2001; Guitton, 2005). In spite of their success, perhaps the most challenging part of working with pattern-based approaches is that they require a model of the patterns of the signal and the noise. For the simultaneous source deblending problem, we overcome this challenge by independently modeling the source wavefields at each iteration of the waveform inversion.

In our waveform inversion scheme, we independently model the sources and use these as models for the unblended data. Upon these models, we estimate non-stationary multidimensional prediction-error filters (PEFs) which then are used as proxies for the spectra of the unblended data in order to approximately deblend the shots. We then update the velocity using gradients calculated on these approximately deblended shots. As the inversion proceeds, the deblending improves and therefore the image contains increasingly fewer artifacts. We show for a linearized waveform inversion (LWI) on the Marmousi model that our proposed algorithm results in an inverted subsurface model with significantly fewer artifacts and one that is comparable to performing LWI on unblended data.

THEORY

Waveform inversion of blended data

A single unblended shot gather observed in recorded seismic data can be mathematically expressed by the following non-linear operation:

$$\mathbf{f}^{u}(\mathbf{m}, \mathbf{x}_i) = \mathbf{d}_i^{u}, \tag{1}$$

where $\mathbf{f}^{u}(\mathbf{m}, \mathbf{x}_i)$ is the unblended non-linear wave equation modeling operator for a particular earth model $\mathbf{m}$ and spatial source location $\mathbf{x}_i$, and $\mathbf{d}_i^{u}$ represents the ith shot gather of a seismic survey. The superscript ^{u} indicates that these data are unblended (never have been blended). With this representation of a single shot gather, we can then form a column vector of non-linear operators to represent n shots and recorded data in

10.1190/segam2018-2997838.1

a single seismic survey as.

$$\begin{bmatrix} \mathbf{f}^u(\mathbf{m},\mathbf{x}_1) \\ \mathbf{f}^u(\mathbf{m},\mathbf{x}_2) \\ \vdots \\ \mathbf{f}^u(\mathbf{m},\mathbf{x}_n) \end{bmatrix} = \begin{bmatrix} \mathbf{d}^u_1 \\ \mathbf{d}^u_2 \\ \vdots \\ \mathbf{d}^u_n \end{bmatrix},$$

$$\mathbf{f}^u(\mathbf{m}) = \mathbf{d}^u. \tag{2}$$

In order to express non-linear blended modeling we introduce the blending operator $\mathbf{\Gamma}$. This operator is linear and its primary function is to describe the blending of the data performed during the acquisition. In matrix form it can be written as a rectangular matrix with many more columns than rows ($n > m$) where the number of rows (m) represents the extent of the blending and the number of columns (n) is determined by the number of shots. Applying this operator to equation 2 results in the following expression

$$\begin{aligned} \mathbf{\Gamma f}^u(\mathbf{m}) &= \mathbf{\Gamma d}^u, \\ \mathbf{f}^b(\mathbf{m}) &= \mathbf{d}^b, \end{aligned} \tag{3}$$

where $\mathbf{f}^b(\mathbf{m})$ and $\mathbf{d}^b$ are the blended non-linear modeling operator and blended data respectively. Now, that we have defined the blended modeling operator and data, we can write the objective function for waveform inversion of blended data as

$$J(\mathbf{m}) = \frac{1}{2}||\mathbf{f}^b(\mathbf{m}) - \mathbf{d}^b||_2^2. \tag{4}$$

It is well known that directly minimizing equation 4 will result in a subsurface model that can be highly contaminated with artifacts. This is due to the fact then when calculating the waveform inversion gradient via the cross-correlation of the source (forward) wavefield and back-propagated data residual (adjoint wavefield) artifacts will be created when the mixed source and receiver wavefields present in the blended wavefields interact (Jiang et al., 2010). While these artifacts can be attenuated with iteration, it can require many iterations to do so and in some cases no amount of iteration will suppress them leading to low-quality seismic images.

Combining direct imaging and data-space deblending

In order to mitigate the strong artifacts contaminating our estimated model parameters, we introduce two primary changes to the traditional blended waveform inversion algorithm. The first of these changes is that as opposed to performing blended modeling, we independently model the source wavefields. The second change is that on these independently-modeled shots we then estimate multidimensional non-stationary PEFs which are then used to deblend the blended data at each iteration of the waveform inversion. With these changes, we can write a modified version of equation 4 as

$$J(\mathbf{m}) = \frac{1}{2}||\mathbf{f}^u(\mathbf{m}) - \mathbf{A}\mathbf{d}^b||_2^2, \tag{5}$$

where $\mathbf{A}$ is a linear filter that is estimated and applied at each iteration of the waveform inversion and has the following property:

$$\mathbf{A}\mathbf{d}^b = \mathbf{d}^d \approx \mathbf{d}^u. \tag{6}$$

This approach of estimating multidimensional non-stationary PEFs on the independently-modeled data (i.e., models for the true unblended data) and then using these PEFs to separate the shots is known as a pattern-based method for signal and noise separation (Abma, 1995). The key to pattern-based approaches is that there exist models for the signal and noise, and that the multidimensional spectra of the signal and noise differ. As previously stated, the first step is to estimate PEFs on the independently-modeled data which can be mathematically expressed as solving the following regressions

$$\mathbf{0} \approx \mathbf{r}_1 = \hat{\mathbf{D}}_1\mathbf{a}_1, \quad \mathbf{0} \approx \mathbf{r}_2 = \hat{\mathbf{D}}_2\mathbf{a}_2,$$

where $\hat{\mathbf{D}}_1$ and $\hat{\mathbf{D}}_2$ are the independently-modeled (proxy) shots formed into convolution operators, $\mathbf{a}_1$ and $\mathbf{a}_2$ are vectors that upon solving these regressions, contain the PEF coefficients and $\mathbf{r}_1$ and $\mathbf{r}_2$ are the prediction-error residuals. While here we have assumed that two shots have been blended, this theory extends to more than just two shots. Note that when solving for these filter coefficients, we force that the zero-lag coefficient be unity in order for these filters to remain PEFs. Upon solving these regressions, the estimated PEF coefficients will contain the approximate inverse spectra of $\hat{\mathbf{d}}_1$ and $\hat{\mathbf{d}}_2$ (Claerbout, 2014). We then form convolution operators ($\mathbf{A}_1$ and $\mathbf{A}_2$) with these filter coefficients and use them in the following objective function in order to deblend the data

$$J(\mathbf{d}^d_1, \mathbf{d}^d_2) = \frac{1}{2}||\mathbf{d}^d_1 + \mathbf{d}^d_2 - \mathbf{d}^b||_2^2 + \frac{1}{2}||\mathbf{A}_1\mathbf{d}^d_1||_2^2 + \frac{1}{2}||\mathbf{A}_2\mathbf{d}^d_2||_2^2, \tag{7}$$

where $\mathbf{d}^d_1$ and $\mathbf{d}^d_2$ are the desired deblended data. The first term of this objective function is the familiar data-space deblending objective function that requires that the sum of the deblended shots be equal to the blended data. The other two terms can be seen as additional constraints and effectively act to enforce the separation of the two shots. Because $\mathbf{A}_1$ and $\mathbf{A}_2$ contain the inverse spectra of $\hat{\mathbf{d}}_1$ and $\hat{\mathbf{d}}_2$, the additional terms constrain $\mathbf{d}^d_1$ and $\mathbf{d}^d_2$ so that they take the spectra of $\hat{\mathbf{d}}_1$ and $\hat{\mathbf{d}}_2$ respectively. We also point out that minimizing equation 7 is equivalent to applying a filter that optimally separates the shots in the least-squares sense (equation 6).

This process of pattern-based deblending occurs at each iteration of the waveform inversion. The key to the waveform inversion with pattern-based deblending algorithm is that it uses both waveform inversion as well as the pattern-based deblending step in order to simultaneously provide high-quality deblended data as well as seismic images. As the subsurface parameters are updated and improved, then so will the deblending at each iteration. We summarize the process of waveform inversion of blended data with pattern-based deblending in algorithm 1.

RESULTS

In order to test our algorithm, we performed a linearized waveform inversion (LWI) on synthetic data generated using the Marmousi velocity model. To create the blended data, we modeled blended data via acoustic finite difference modeling where each blended shot consisted of two shots with randomly dithered shot times and a 1.4km shot spacing. In total, we had 23 blended shots with receivers at each grid point on the surface.

10.1190/segam2018-2997838.1

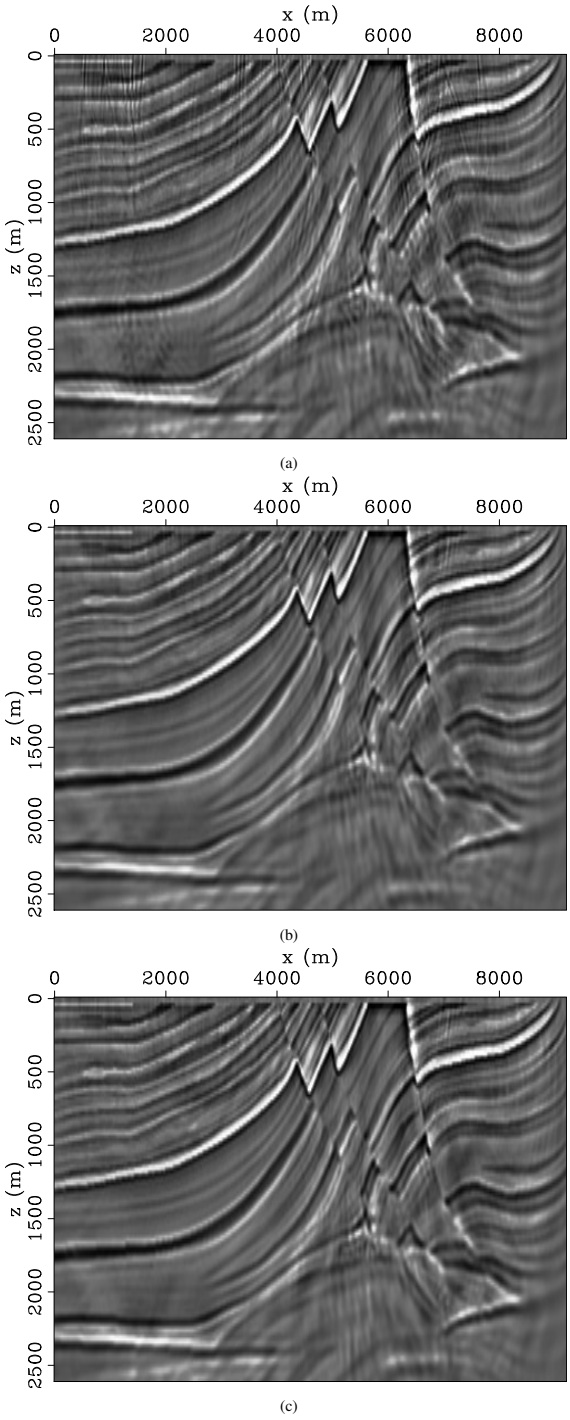

Figure 1: Comparison of (a) direct LWI of blended data, (b) LWI with a pattern-based method and (c) conventional LWI. Note that the image resulting from direct LWI of blended data (panel (a)) is contaminated with a number of artifacts. Also note that using the pattern-based method with LWI results in a clean image that is comparable to LWI of unblended data.

Algorithm 1 Waveform inversion of blended data with pattern-based deblending

Require: $\mathbf{m}_0$ (starting/background model) and $\mathbf{d}^b$

1: **for** iter=0 < n_iter; iter++ **do**
2: Compute independently-modeled data $\mathbf{f}^u(\mathbf{m}_{iter}) = \hat{\mathbf{d}}_{iter}$
3: Estimate non-stationary, multidimensional PEFs on $\hat{\mathbf{d}}_{iter}$
4: With the PEFs, deblend $\mathbf{d}^b$ via the minimization of equation 7 resulting in the deblended data $\mathbf{d}^d_{iter}$
5: Compute the data residual: $\mathbf{r}_{iter} = \hat{\mathbf{d}}_{iter} - \mathbf{d}^d_{iter}$
6: Compute gradient using $\mathbf{r}_{iter}$
7: Update model with gradient
8: **end for**

Using a smoothed version of the true Marmousi model as our background velocity model ($\mathbf{m}_0$), we then performed 30 iterations of LWI with pattern-based deblending as well as 30 iterations of blended LWI. The results of these inversions are shown in Figure 1. Comparing the results of blended LWI (Figure 1a) with those of LWI with pattern-based deblending (Figure 1b) we observe that the inverted result from LWI with pattern-based deblending has significantly fewer artifacts. In fact, the inverted result from LWI with pattern-based deblending is comparable to the result obtained from LWI of unblended data shown in Figure 1c.

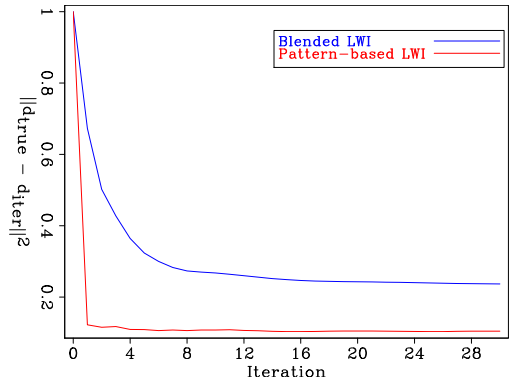

Figure 2: Comparison of convergence of deblended data obtained from blended linearized waveform inversion (blue curve) and deblended data obtained from the iterative deblending performed during the LWI with the pattern-based approach (red curve). Note that after 30 iterations direct imaging of the blended data only provides deblended data within approximately 25% of the true data whereas using the pattern-based approach brings the error down to approximately within 10%.

Next we compared the deblended data obtained using each approach. To obtain the deblended data from the blended LWI, we performed independent modeling (after completing the inversion) on the estimated models from each iteration. For our LWI with pattern-based deblending, we used the deblended data at each iteration of the LWI. Figure 2 shows the convergence of the deblended data from each algorithm to the true unblended data. The blue curve shows the convergence of

10.1190/segam2018-2997838.1

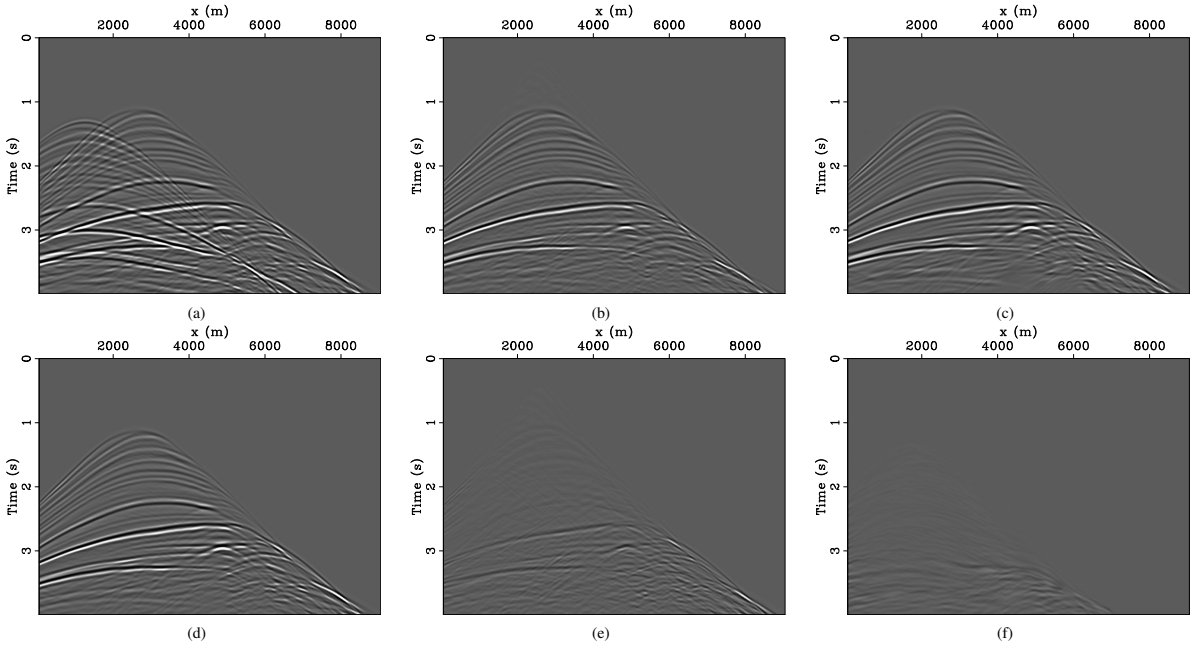

Figure 3: Comparison of deblended data obtained from blended LWI and LWI with a pattern based approach. (a) Two blended shots, (b) the deblended shot obtained via linearized modeling after 30 iterations of blended LWI. (c) The deblended shot after 30 iterations of LWI with a pattern-based approach, (d) the true unblended data, (e) the difference between (b) and (d) and (f) the difference between (c) and (d). Note in panel (e) that there remains signifiant residual noise due to slow convergence in fitting the data.

blended LWI and the red shows the convergence of LWI with pattern-based deblending. When comparing the two curves, it is clear that the pattern-based approach demonstrates superior convergence. Additionally, we observe from the convergence of LWI with pattern-based deblending that the filtering improves slightly with iteration. This shows that indeed both inversions (equations 5 and 7) are working togeher thus providing faster convergence than conventional blended LWI.

Figure 3 shows the deblended data from both blended LWI and LWI with pattern-based deblending. Note that while both algorithms successfully deblend the data, the difference between the deblended and unblended data shown in Figures 3e and 3f shows again that using the pattern-based deblending results in a deblended data that is closer to the unblended data. In terms of the signal to noise ratio (SNR) defined as

$$\text{SNR} = \frac{||\mathbf{d}^u||_2^2}{||\mathbf{d}^u - \mathbf{d}^d||_2^2}, \tag{8}$$

we find that the deblended data obtained from blended LWI has an SNR of 7.10 dB whereas the deblended data obtained from LWI with pattern-based deblending has an SNR of 10.65 dB.

In spite of this increased performance, when compared to direct imaging of blended data, our proposed algorithm is more computationally demanding due to the need for the independent modeling of the shots. However, our algorithm requires approximately the same computational cost as traditional waveform inversion as the data-space deblending step is negligible when compared to the compuational cost of an iteration of waveform inversion.

CONCLUSION

We presented a new algorithm for directly imaging simultaneous source blended data that uses a computationally inexpensive data-space deblending step at each iteration of the waveform inversion. This data-space deblending step is performed using a pattern-based approach that requires that we independently-model the source wavefields. Filters then are estimated on these independently-modeled data and then are used to deblend the blended data at each iteration of the waveform inversion. We showed for a linearized waveform inversion example on the Marmousi model that introducing the pattern-based deblending at each iteration resulted in an inverted subsurface model with fewer artifacts and deblended data with more reliable amplitudes. For future work, we plan to move beyond the linearized-waveform inversion example and solve the full-waveform inversion problem with pattern-based deblending.

ACKNOWLEDGEMENTS

We thank the affiliates of the Stanford Exploration Project for their support and the other students and professors at Stanford for their help and advice.

10.1190/segam2018-2997838.1

REFERENCES

Abma, R. L., 1995, Least-squares separation of signal and noise with multidimensional filters: Ph.D. dissertation, Stanford University.

Abma, R. L., and J. Yan, 2009, Separating simultaneous sources by inversion: 71st Annual International Conference and Exhibition, EAGE, Extended Abstracts, V002, https://doi.org/10.3997/2214-4609.201400403.

Abma, R. L., Q. Zhang, A. Arogunmati, and G. Beaudoin, 2012, An overview of BP's marine independent simultaneous source field trials: 82nd Annual International Meeting, SEG, Expanded Abstracts, 1–5, https://doi.org/10.1190/segam2012-1404.1.

Beasley, C. J., R. E. Chambers, and Z. Jiang, 1998, A new look at simultaneous sources: 68th Annual International Meeting, SEG, Expanded Abstracts, 133–135, https://doi.org/10.1190/1.1820149.

Berkhout, A. J., 2008, Changing the mindset in seismic data acquisition: The Leading Edge, **27**, 924–938, https://doi.org/10.1190/1.2954035.

Brown, M., R. G. Clapp, and K. Marfurt, 2001, Predictive signal/noise separation of ground-roll-contaminated data: Stanford Exploration Project, Report 102, 1–128.

Chen, Y., H. Chen, K. Xiang, and X. Chen, 2017, Preserving the discontinuities in least-squares reverse time migration of simultaneous-source data: Geophysics, **82**, no. 3, S185–S196, https://doi.org/10.1190/geo2016-0456.1.

Claerbout, J., 2014, Geophysical image estimation by example: Lulu.com.

Guitton, A., 2005, Multiple attenuation in complex geology with a pattern-based approach: Geophysics, **70**, no. 5, V97–V107, https://doi.org/10.1190/1.1997369.

Jiang, Z., and R. Abma, 2010, An analysis on the simultaneous imaging of simultaneous source data: 80th Annual International Meeting, SEG, Expanded Abstracts, 3115–3119, https://doi.org/10.1190/1.3513493.

Kommedal, J., G. Alexander, S. Wagner, and L. Wyman, 2016, ISS on ice: Seismic acquisition in the arctic: 86th Annual International Meeting, SEG, Expanded Abstracts, 6–10, https://doi.org/10.1190/segam2016-13866643.1.

Leader, C., 2015, The separation and imaging of continuously recorded seismic data: Ph.D. dissertation, Stanford University.

Manin, M., and S. Spitz, 1995, 3D attenuation of targeted multiples with a pattern recognition technique: 57th Annual International Conference and Exhibition, EAGE, Extended Abstracts, B046, https://doi.org/10.3997/2214-4609.201409343.

Soni, A. K., and D. J. Verschuur, 2015, Imaging blended vertical seismic profiling data using full-wavefield migration in the common-receiver domain: Geophysics, **80**, no. 3, R123–R138, https://doi.org/10.1190/geo2014-0193.1.

Tang, Y., and B. Biondi, 2009, Least-squares migration/inversion of blended data: 79th Annual International Meeting, SEG, Expanded Abstracts, 2859–2863, https://doi.org/10.1190/1.3255444.

Xue, Z., Y. Chen, S. Fomel, and J. Sun, 2016, Seismic imaging of incomplete data and simultaneous-source data using least-squares reverse time migration with shaping regularization: Geophysics, **81**, no. 1, S11–S20, https://doi.org/10.1190/geo2014-0524.1.